Nanophotonics 1 (2012): 235–248 © 2012 Science Wise Publishing & De Gruyter • Berlin • Boston. DOI 10.1515/nanoph-2012-0180

Review

Nanoplasmonics: a frontier of photovoltaic solar cells

Min Gu[1,*], Zi Ouyang[1], Baohua Jia[1,*], Nicholas Stokes[1], Xi Chen[1], Narges Fahim[1], Xiangping Li[1], Michael James Ventura[1] and Zhengrong Shi[2]

[1] Centre for Micro-Photonics, Faculty of Engineering and Industrial Sciences, Swinburne University of Technology, P.O. Box 218, Hawthorn, 3122 Victoria, Australia, e-mail: mgu@swin.edu.au; bjia@swin.edu.au
[2] Suntech Power Holdings Co., Ltd., 9 Xinhua Road, New District, Wuxi, Jiangsu Province 214028, China

*Corresponding authors

Abstract

Nanoplasmonics recently has emerged as a new frontier of photovoltaic research. Noble metal nanostructures that can concentrate and guide light have demonstrated great capability for dramatically improving the energy conversion efficiency of both laboratory and industrial solar cells, providing an innovative pathway potentially transforming the solar industry. However, to make the nanoplasmonic technology fully appreciated by the solar industry, key challenges need to be addressed; including the detrimental absorption of metals, broadband light trapping mechanisms, cost of plasmonic nanomaterials, simple and inexpensive fabrication and integration methods of the plasmonic nanostructures, which are scalable for full size manufacture. This article reviews the recent progress of plasmonic solar cells including the fundamental mechanisms, material fabrication, theoretical modelling and emerging directions with a distinct emphasis on solutions tackling the above-mentioned challenges for industrial relevant applications.

Keywords: nanoplasmonics; photovoltaic solar cell; broadband light trapping; nanofabrication; metal nanostructure.

1. Introduction

Energy requirements and climate change are two major threads for the sustainability of the human community. Photovoltaics (PV) solar energy has been widely considered as one of the most promising technologies that address both issues. PV directly converts solar energy into electricity, which allows the efficiency of PV to be fundamentally and practically higher than other indirect processes of transforming solar energy to electricity, such as solar-photosynthesis-fuel-electricity [1] and solar-thermal-electricity [2]. Importantly, CO_2 and other pollutants are not involved in the PV conversion rendering it a totally green process. Although playing an increasingly important role in the world's energy market, PV is limited by its low energy density, which is the power release per unit volume, mass or time. Such a limit constrains the usability of PV devices, and results in high production and implementation costs. Therefore, increasing the efficiency, which is the generated power per unit area, has always been the most important research topic, since the first PV device was demonstrated in 1839 and the first modern device was reported in 1954 [3].

A PV process includes (i) absorption of photons, (ii) energy transfer from photons to electron-hole pairs, and (iii) transport of the charges to external loads. Higher overall energy conversion efficiency requires higher efficiency at each step. Because of the lasting development of the semiconductor industry and extensive PV R&D, close-to-unity internal quantum efficiency and negligible resistive losses of modern solar cells indicate that Steps (ii) and (iii) have already been highly efficient [4]. Relatively, Step (i) provides a much larger room for ultra-high efficient PV devices. However, this requires ground-breaking light trapping fundamentals to overcome the limited light absorption enhancement predicted based on the conventional Lambertian scattering theory [5, 6], which has already been approached by modern micro-scale light trapping technologies such as surface texturing, anti-reflection coating (ARC) and back-surface reflectors (BSR).

Sub-wavelength light trapping structures, which can induce nanophotonic and nanoplasmonic modes, demonstrated great opportunities to exceed the conventional limits set by the micro-scale ray optics [7, 8]. Nanoplasmonic structures in particular, due to their capability to strongly localize and reconstruct the electromagnetic field, have been extensively researched for PV light trapping, since the late 1990s [9].

This paper reviews the state-of-the-art of nanoplasmonics as a frontier of highly efficient PV solar cells. It includes the fundamentals and design considerations of plasmonic solar cells, popular computing methods for plasmonic nanostructures and PV device modeling, various fabrication technologies for plasmonic PV devices, the most recent progress in plasmonic PV and the emerging nanoplasmonic technologies. Practical considerations are discussed in particular, such as possibilities of combining plasmonics with other light trapping methods, realistic ways of modifying the solar module production line to incorporate plasmonic structures, a trade-off between the fineness of plasmonic structures and the complexity of device fabrication, etc. In this paper, we cover both fundamental and practical aspects of the nanoplasmonic PV technologies.

2. Fundamentals and design considerations

Surface plasmons are coherent electron oscillations at the interface of two materials with opposing dielectric functions. They can be effectively excited at the metal-dielectric interface by interacting with the incident light, resulting in changes of the orientation and spatial concentration of the light. With carefully designed nanostructures, plasmons can improve the performance of PV devices by (i) guiding and (ii) concentrating the light for enhanced absorption. To date, most of the reported designs fall into one, or both of the categories, as summarized in Table 1.

2.1. Guidance direction of light

From a ray optics point of view, guiding the light towards larger refraction angles, θ, can significantly increase the effective light path length in the active layer and therefore creates a larger probability for the light to be absorbed. Firstly, in a single light path through the active layer, the effective path length is increased from the layer thickness, L, to $[1+\cos(\theta)]\times L$. More importantly, if the angle is larger than the critical angle of total internal reflection at the active layer-outer layer interface, the light does not escape from the active layer but bounce back-and-forth in the sandwich structure with low-high-low refractive index. For a fully-randomized (Lambertian) scatterer, the passes can be enhanced as high as $4n^2$ folds, where n is the refractive index of the active layer [5]. The significance of such a scattering effect is demonstrated in Figure 1 (A), where the absorption of a 2-μm crystalline Si (c-Si) film with and without the Lambertian scatterer is compared. Under the standard air mass 1.5 spectrum conditions, the number of absorbed photons and consequently the maximum photocurrent are doubled with such an ideal scatterer [28]. From a wave optics point of view, a limit-breaking light trapping scheme would have to strongly couple the incident light into modes and maximize the ratio of light that is coupled in to out. It requires the electromagnetic local density of optical states (LDOS) over the active layer is higher than the LDOS of the bulk material [8]. If the evanescent mode at the interface can be effectively trapped for electron-hole pair generation, the enhancement margin could be even greater [29].

Nanoplasmonic structures can be very effective light scatterers [30]. By the finite-difference time-domain (FDTD) calculation of a first-order scattering mode, plasmonic nanostructures were predicted to have significant enhancements of the light path length, as shown in Figure 1(B) [31]. The maximum light path enhancement of the electric point dipole even exceeds the Lambertian limit. For the most effective plasmonic light scattering for photocurrent enhancement in a PV device, three aspects need to be carefully considered; (i) scattering pattern, (ii) dissipated absorption of light in the metal nanostructures and (iii) spectrum selectivity. Firstly, for the scattering pattern of nanostructures on the *front* surface of a PV device, it is preferred that more photons to be scattered (larger scattering cross section) forward into the substrate (less reflection), and to have a "flatter" scattering pattern (scattering to larger angles). When an optimized scatterer is designed, it should be noted that trade-offs between the three aspects usually exist and a balance is needed. Noticeably, for nanostructures on the *rear* side of a device with an additional back reflector, the forward or backward scattering is not a consideration any more, as essentially all the light is reflected back to the active layer by either the plasmonic nanostructures or the BSR. This usually gives more freedom for the design. Secondly, the dissipated absorption of light in the metal nanostructures at the surface plasmon resonance (SPR) wavelengths can be significant. Since this fraction of energy eventually transforms into heat instead of electricity, it needs to be minimized in any circumstance. Thirdly, scattering is the strongest at the SPR peak and decreases considerably off-peak. On the one hand, this feature is useful as one can tune the SPR peak to the wavelengths where the enhanced light absorption is most demanding; on the other hand, the narrow spectrum selectivity of plasmonics is a hurdle to achieve broadband enhancement over the entire important spectrum. This disadvantage generally exists for any sub-wavelength light trapping mechanism and it has to be overcome [7, 32]. Based on these design principles, numerous computational and experimental studies have been reported on tuning the metal material, the shape, size and packing density, the dielectric environment and the position of the plasmonic nanostructures in PV devices to achieve enhanced light absorption for various types of solar cells [10, 13, 15, 24, 31–38].

Due to the position change of the sun and light scattering in the earth's atmosphere, in real life a considerable amount of incident light strikes at the solar device with an angle off the normal direction. Therefore, merely looking into the normal incident light is not enough and it is important to interrogate the angular-dependent performance of a light trapping scheme [39]. While some theoretical investigation has been conducted on plasmonic nanostructures and fairly positive results have been demonstrated [40], other research has predicted the "super-Lambertian" enhancement for normal incident light must pay the expense of less enhancement at other angles [39]. Therefore, an integrated evaluation of a plasmonic scheme over all the incident angles is essential but remains as a challenge. One has to consider at least two factors: (i) the angular-dependent light intensity in the solar irradiation. Generally, the larger the incident angle is, the weaker the light intensity becomes. (ii) The responsivity of the solar cell to light intensity. For example, thin-film solar cells in general have better low-light response than the c-Si wafer solar cells. These two factors assign different importance to different incident angles, which in turn affects the design of plasmonic light trapping to achieve maximum energy outcome overall.

2.2. Metal absorption elimination and broadband light enhancement

Since the resonant scattering almost happens at the same wavelength to the resonant absorption, the enhancement from light scattering could be partially or totally offset by the detrimental dissipated absorption in the metal. Several methods have been proposed to resolve this issue: careful selection

Table 1 Recent progress in nanoplasmonic photovoltaic devices. (*PC* stands for photocurrent, *Eff* for efficiency and λ for wavelength.)

Mechanism	Solar cell type	Plasmonic material and location	Fabrication method	Enhancement (relative)	Enhancement (absolute)	Reference
Light direction guidance (far-field) 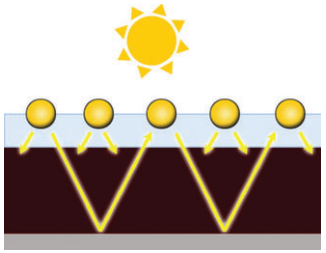	300 µm planar wafer c-Si	Ag NPs, front	Deposition + annealing	Absorption 700% at λ=1200 nm	N/A	[10]
	400 µm planar wafer c-Si	Ag NPs, rear	Deposition + annealing	*PC* 16%[1] at λ=900-1200 nm	*PC*: 1.1 mA/cm^2	[11]
	22 µm planar c-Si	Ag NPs, rear	Deposition + annealing	*PC* 10%	N/A	[12]
	multi-Si wafer, commercial	Au NPs, front	Chemical synthesis + dip coating	*PC* 11% at λ=1150 nm, *Eff* 2%	*Eff* from 14.9% to 15.2%	[13]
	c-Si wafer, commercial	Ag NPs, front	Electroless displacement	*Eff* 35.2%	*Eff* from 11.2% to 15.2%	[14]
	a-Si thin-film, substrate-configured	Au NPs, front	Synthesis + coating	*PC* 8.1%, *Eff* 8.3%	*PC* from 6.66 to 7.2 mA/cm^2, *Eff* from 2.77% to 3%	[15]
	a-Si thin-film, substrate-configured	Ag NPs, rear	Deposition + annealing	*PC* 20%	*PC* from 10.07 to 12.12 mA/cm^2	[16]
	a-Si thin-film, substrate-configured	Ag nanostructure, rear	Nanoimprinting lithography	*PC* 47%, *Eff* 15%[2]	*PC* from 11.52 to 16.94 mA/cm^2, Eff from 6.32% to 9.6%	[17]
	a-Si thin-film, superstrate-configured	Ag NPs, rear	Synthesis + coating	*PC* 14.3%, *Eff* 23%	Highest *Eff* 8.1%	[18]
	GaAs	Ag NPs, front	Evaporation through anodic Al template	*PC* 8%, *Eff* 25%	*PC* from 11 to 11.9 mA/cm^2, *Eff* from 4.7% to 5.9%	[19]
	Organic, P3HT:PCBM	Ag NPs, front	Synthesis + spin coating	*PC* 58%, *Eff* 69%	*PC* from 4.6 to 7.3 mA/cm^2, *Eff* from 1.3% to 2.2%	[20]
	Organic, P3HT:PCBM	Au NPs, front	Electrostatic assembling	*PC* 36%, *Eff* 20%	*PC* from 10.74 to 11.13 mA/cm^2, *Eff* from 3.04% to 3.65%	[21]
Light concentration (near-field) 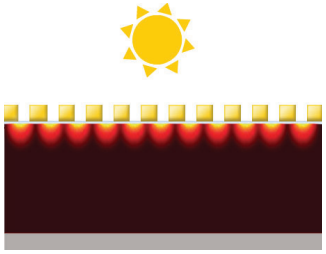	a-Si thin-film	Ag nanowire array, front	(Numerical simulation)	*PC* 60% (calculated)	N/A	[22]
	a-Si/c-Si heterojunction	Au NPs, front	Sputtering on heated substrate	*PC* 20%, *Eff* 25%	*PC* from 19 to 22.9 mA/cm^2, *Eff* from 7.5% to 9.4%	[23]
	poly-Si thin-film, superstrate-configured	Ag NPs, rear	Deposition + annealing	*PC* 44%[3]	*PC* from14.85 to 21.42 mA/cm^2	[24]
	InGaN	Ag NPs, embedded	(Numerical simulation)	*Eff* 27% (calculated)	*Eff* from 10.59% to 13.53% (calculated)	[25]
	Organic, CuPc-PTCBI tandem	Ag clusters, at interface of two sub-cells	Deposition	*PC* 29%, *Eff* 26% (calculated)	*PC* from 3.65 to 4.72 mA/cm^2, *Eff* from 1.9% to 2.4% (calculated)	[26]
	Organic, polymer/PCBM	Al gratings	Nanoimprinting lithography	Absorption enhanced	N/A	[27]

[1]With an additional detached Ag mirror BSR. [2]The Ag nanostructure acts as plasmonic BSR, and it also causes uneven active layers of the cells, which also scatters the light. [3]With an additional white paint BSR. Ag NPs have direct contact with the active layers of the cells.

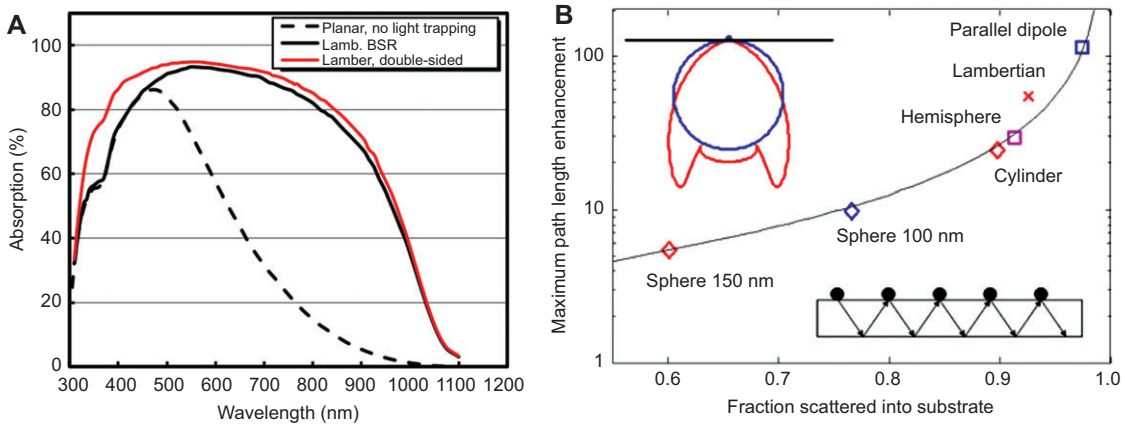

Figure 1 (A) Ray-optical modelling of the light absorption of a 2-μm thick c-Si film without light enhancement management (black dash-line), with a Lambertian back surface reflector (BSR, black solid-line) and a double-sided Lambertian scatterer (red solid-line) [28]. (B) Maximum path-length enhancement and fraction of photons forward-scattered into the substrate of conventional Lambertian scatterer and nanoplasmonic scatterers. (Reprinted with permission from Catchpole KR, Polman A. Design principles for particle plasmon enhanced solar cells. Appl Phys Lett 2008**,** 93, 191113–3. © 2008 American Institute of Physics.)

of the metal element and the structure volume can achieve a relatively large scattering cross section and a small absorption cross section, increasing the scattering/absorption ratio of the metal nanostructure [30, 41]; when the metal nanostructures are coated with dielectric materials, the absorption peak can shift away from the scattering peak to insignificant wavelengths, leaving the scattering peak at the important wavelengths for maximum light enhancement [42, 43]; rear-located nanostructures in a PV device do not suffer from the dissipated absorption of the short wavelength light in the metal, as this range of light is absorbed by the solar cell active layer during the its first pass through it [12, 16, 18, 24, 36–38, 44]; we recently reported that by using a nanomaterial (such as Al) whose SPR wavelength is shorter than the lower end of the absorption band of the PV device, the metal absorption can be minimized and the forward scattering can still be mostly preserved [45]. For PV devices with heavily damped semiconductors, their active layers are able to compete with unwanted metal absorption. To maximize this favorable feature the plasmonic structure needs to be placed close to the active layer. Details are discussed in Section 2.3 as local concentration of light is introduced.

All the designs that have been proposed to realize broadband nanoplasmonic scattering are based on the combination of light trapping components with different resonance wavelengths. One popular suggestion is to mix multiple types of nanoparticles, with distinct resonances, over the device surface [24, 38, 46]. However, there is an obvious limit to this process in that geometrically each nanoparticle can only occupy one place on the surface. This results in narrowband enhancement for each individual particle only providing "diluted" broadband enhancement by combining many particles over a large area. After the integration over the entire surface area, the overall enhancement from a mixed arrangement of nanoparticles is not likely to be considerably better than that from a singular arrangement. In fact, measured advantages of this mixed arrangement have not been reported. To surpass this geometrical limit, the enhancement has to be uniformly broadband at every occupied position.

We recently developed a type of nucleated Ag nanoparticle, where each nanoparticle contains small particle components and a large particle component that can effectively scatter the light of broadband, as shown in Figure 2. When the nucleated nanoparticles were integrated on the rear surface of superstrate *p-i-n* amorphous Si (a-Si) thin film solar cells, as high as 14.3% photocurrent enhancement and 23% efficiency enhancement were achieved, resulting in 8.1% efficient solar cells [18]. This model opened a new path for the design of broadband light scattering.

2.3. Local concentration of light and surface plasmon polariton

The metal nanostructures can trap the electromagnetic field in their close approximation by resonant plasmon excitation. Figure 3 demonstrates an unchanged electric field surrounding a nanosphere when the frequency of the incident light is off the SPR frequency, and a concentrated near-field when the light frequency is on the SPR peak. By overlapping the near-field (a few tens of nanometers) with the PV active layer, the highly localized field can excite more electron-hole pairs locally without the need to let the photons travel too far. Numerical simulation demonstrates that the near-field enhancement is significantly beneficial for the InGaN-based solar cells by embedding the nanoparticles in the active layer [25]. Such strong-absorbing direct bandgap semiconductor materials are particularly suitable for the design of the plasmonic local concentration, as the active layer is more preferable over the metal nanostructure in terms of competition for the energy absorption. It is also found through simulations that heavily damped, ultra-thin semiconductor materials such as $CuInSe_2$, a-Si and organic MDMO-PPV are advantageous

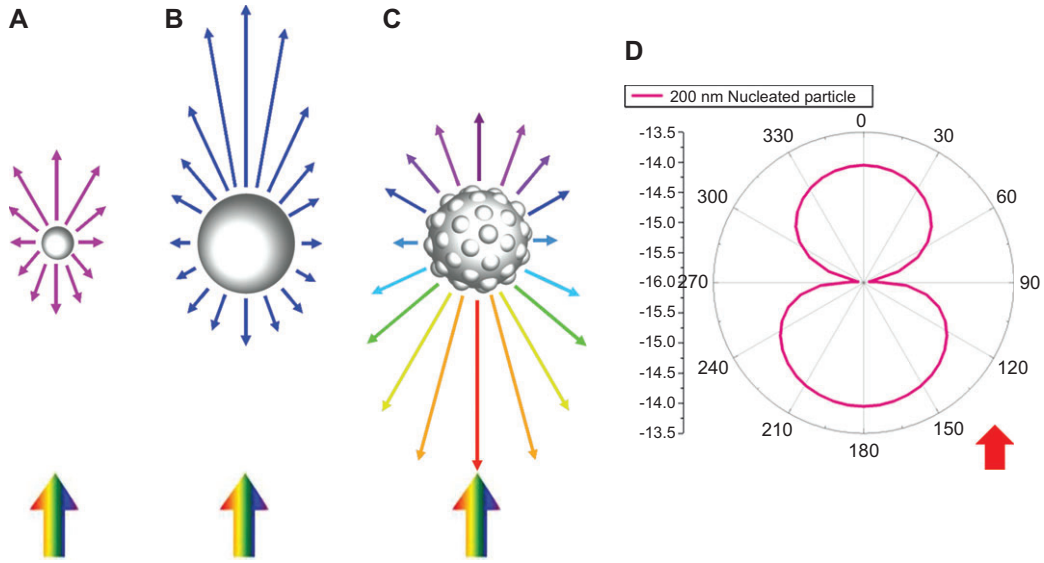

Figure 2 Schematic drawings showing the scattering patterns of (A) a small nanoparticle; (B) a large nanoparticle of 200 nm; (C) a nucleated large nanoparticle of 200 nm; and (D) the calculated scattering intensity vs. scattering angle pattern for a nucleated large nanoparticle of 200 nm under the illumination of a total-field-scattered-field plane wave from 300 to 800 nm with the FDTD method. (Reprinted with permission from Chen X, Jia B, Saha JK, et al. Broadband Enhancement in Thin-Film Amorphous Silicon Solar Cells Enabled by Nucleated Silver Nanoparticles. Nano Lett 2012, 12, 2187–92. © 2012 American Chemical Society.)

in the absorption competition with relatively lowly damped metal nanoparticles [47, 48]. In the practical design of a PV device, the contact between the metal and the semiconductor active layer is generally unfavorable due to the increase of the recombination states at the interface, and therefore a so-called dielectric passivation layer is necessary [49, 50], which intercepts the effective overlap between the near-field and the active layer. However with this trade-off taken into account, some types of solar cells may still take advantage of the close contact between the plasmonic structure and the semiconductor active layer. First category is ultra-thin solar cells having highly damped active layers. The optical gain due to light concentration is much larger than the electrical loss due to recombination, resulting in an optimum barrier thickness of a few nanometers [48]. This barrier can be realized by means of coating the semiconductor with a dielectric layer or coating the metal nanostructure with a dielectric shell [51]. The second category includes low-purity semiconductor materials. The bulk recombination is so high that the surface passivation is unnecessary, and the contact between metal and the active layer only results in beneficial near-field enhancement, and does not cause noticeable performance degradation. Take one such "low quality" material, the evaporated thin-film polycrystalline Si for example, the light absorption and solar cell efficiency tend to be significantly improved when the dielectric spacing layer was reduced and finally removed, enabling near-field enhancements [24, 44].

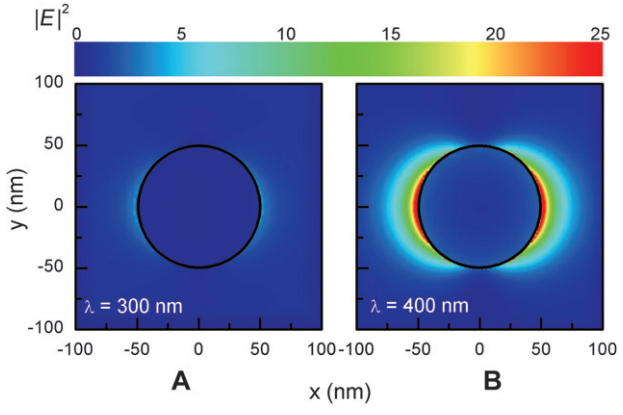

Figure 3 An electric field intensity map of a 100 nm diameter Ag nanoparticle in vacuum (A) off resonance at 300 nm wavelength and (B) on resonance at 400 nm.

Periodic metal nanostructures on the surface of a PV device can excite surface plasmon polariton (SPP) modes. In SPP modes, the waves are guided and propagate horizontally along the metal nanostructure, where the energy can be absorbed in the adjacent semiconductor layer to generate electron-hole pairs [40, 52, 53]. However, similar to the case of the near-field effect, the competition between the dissipated absorption in the metal and the absorption in the semiconductor active layer needs to be considered. It was calculated for the weakly-absorbing, indirect bandgap c-Si, more than half of the light in the range of 600–1200 nm is absorbed by the Al or Ag nanostructures instead of the Si, although the fraction absorbed in the semiconductor could be higher for GaAs and some high-absorbing organic materials [9]. In fact, SPP modes were suggested to act as an efficiency loss mechanism, instead of an enhancement mechanism, for Si solar cells [17, 54–56].

The dissipated absorption of metal at a continuous metal-semiconductor interface seems to be a general difficulty for many light trapping designs. Another example is the surface texturing technology for c-Si wafer solar cells. If the metal BSR is not absorbing, the rear-surface texturing as a scattering mechanism tends to enhance the light absorption in the Si wafer [6]. But in the highly-efficient solar cell fabrication process the rear surface is always polished to reduce the light absorption in Al close to the Al-Si interface [57].

3. Plasmonic solar cell modeling

Interactions of plasmonic nanomaterials in combination with solar cells have been simulated utilizing several different computational methods. These methods include the Finite-Difference Time-Domain (FDTD) method [18, 31, 40, 44, 45, 53, 58–61], the Finite-Difference Frequency-Domain (FDFD) method [53, 61], the Finite Element Method (FEM) [15, 26, 62–64], and the Fourier Modal Method (FMM) [22]. Computational simulations have been used to investigate some of the following characteristics of plasmonic materials and solar cells; scattering, absorption and extinction cross-sections, absorbed power, cell reflectance and transmittance, optical path length, absorption enhancements, electric field distributions and short circuit current of solar cells if the internal quantum efficiency is given.

Among various methods, the FDTD method, also called the Yee algorithm, is probably the most popular one in terms of the number of reported results. This modeling technique is used to solve the Maxwell's equations, in differential form over a grid-based domain [65]. It is a time-domain technique, which allows solutions to be obtained for a wide range of frequencies in a single simulation. Since the FDTD method calculates the electric, E, and magnetic, H, fields everywhere in the computational domain as they evolve in time, it is straightforward to simulate the electromagnetic field movement through the model [66]. There are many commercially available FDTD software vendors [67], which are easy-to-use and can simulate 2D and 3D cases. The published FDTD research outcomes include the investigation of nanostructure shape, material, dielectric environment, array pitch and location in the cell structure with regard to the scattering into the substrate [18, 31, 37, 44, 45, 59, 60, 68].

The FDFD method shares many similarities to the FDTD method but works by transforming the Maxwell's equations in linear media for sources and fields at a constant frequency instead of time. Although powerful, finite difference methods are limited in their modeling capability due to their grid-based nature. Geometries are approximated using a discrete grid, which must be sufficiently sized to resolve both the smallest electromagnetic wavelength and the smallest geometrical feature in the model, which may result in computationally intense solutions [66].

The FEM is used for finding the approximate solution of partial differential equations and integral equations. The FEM is suitable for modeling irregular geometries as well as large domains containing fine details and is accomplished by using small elements in regions where materials or fields are expected to change abruptly and simulating larger elements in the less important regions [66]. The COMSOL Multiphysics software [69], which uses the FEM, was applied to design plasmonic nanostructures for maximum performance enhancement of various PV devices [15, 26, 62, 63, 70–72].

The FMM divides the structure into layers with no variation in the material properties along the principle propagation direction. In each layer all physical quantities are expanded into a Fourier series and the Bloch periodic eigenmodes in each layer are subsequently calculated. The amplitude of each mode is found by imposing appropriate boundary conditions among each layer and once the amplitudes are known, the electric field can be calculated everywhere in space [22].

The abundance of computational methods that have been mentioned here has specifically been used to model plasmonic solar cells or major aspects. Moreover, there are many more methods available when investigating isolated aspects of the plasmonic solar cells such as investigating the optical response of the nanoparticles. Selecting which computational method to use depends on what the desired output is. In general, the FDTD method is able to provide a relatively thorough model of the simulated plasmonic solar cells over the required frequency range in a single calculation and with results including the absorption, transmission, reflectance and the scattering cross-section obtainable.

Based on the optical computational methods, simulation of the final power conversion efficiency of nanoplasmonic solar cells is one important step further. A simple way is using the active layer absorption resulting from the optical simulation as input parameters to semiconductor or solar cell device simulators, such as ATLAS [73] and PC1D [74]. In the cases where the near-field effect is significant or the nanostructures are embedded in the active layer of a solar cell, the distribution profile of the photons absorbed and the electron-hole pair recombination rate can be dramatically modified by the nanostructures. In order to achieve accurate simulation under such circumstances, both the absorption profile and corresponding internal quantum efficiency (as a function of the spatial position, photon density and frequency) are needed. In the cases where the nanostructures can help to transport the electrons [9, 19], the series resistance reduction and fill factor enhancement for a solar cell needs to be considered as well.

4. Fabrication technologies

Directed by theoretical design principles and computational simulation results, various fabrication technologies have been developed for realizing nanoplasmonic solar cells, as summarized in Table 2. There are physical deposition methods, chemical synthesis methods and combinations of both. (i) Fabrication feasibility and (ii) cost-effectiveness are two essential criteria for screening fabrication technologies, although the emphasis may be at different levels for lab research and mass production. From the feasibility point of view, the

Table 2 Fabrication methods of nanoplasmonic functional structures

	Fabrication method	Advantages	Disadvantages
Random structures	Deposition + annealing	Simple and capable of upscale for in-line mass production, inherent capability of producing hemispherical nanoparticles.	Limited control of nanoparticle size and surface arrangement, incapable to fabricate complex nanostructures, vacuum is usually needed.
	Deposition through a patterned mask (e.g., anodic Al template)	Good control of nanostructures, no high temperature process involved.	Poor reliability and low lifetime of the masks limit the mass production.
	Electrodeposition	High nanoparticle packing density on the surface, ignorable metal material wastes.	Particle size relatively small, incapable of fabricating complex nanostructures, poor uniformity over a large surface.
	Chemical synthesis + a coating method	Good and independent control of nanoparticle size, shape and surface arrangement, capable of mass production.	Limited capability of fabricating complex nanostructures.
	Laser ablation from solution	Simple process.	Incapable of fabricating complex nanostructures, low throughput.
Ordered structures	Direct pattern writing by electron beam lithography or ion beam lithography	Very fine control of nanostructures, 3D nanostructures producible.	Very low throughput, very high cost.
	Nanoimprint lithography	Fine control of nanostructures by replica, capable of roll-to-roll mass production.	Patterns cannot be faithfully transferred for very rough device surfaces, medium cost level.

nanostructure fabrication process has to be integrated as a part of the entire cell fabrication process. Taking temperature tolerance for an example, metal nanostructure integration should not be prior to the back surface field (BSF) formation process of c-Si wafer solar cells, as the formation of BSF requires high temperature that can destroy most of the metal nanostructures; laser direct writing or other nanostructure fabrication methods, which can introduce high-temperature to the PV device during integration, are not suitable for a-Si solar cells, as the amorphous Si tends to be crystallized at 600°C or above [75]. In regards to the economic factor, it is generally believed that the cost of PV has to be cheaper than US\$1/W_p in order to make the solar electricity competitive with conventional sources of electricity [76–78], although recently the cost has been cut down abruptly due to the abundant supply of silicon feedstock. According to the solar electricity costs predicted in the literature [77, 78], we believe that the add-on cost of every 1% efficiency enhancement (absolute) should not exceed ~ \$10/m^2; otherwise, the gain from the improved efficiency is completely offset by the increased cost. The cost of \$10/m^2 per 1% efficiency enhancement can be considered as an economic boundary for the design of plasmonic nanostructures for improved PV devices.

4.1. Random structures

There is a general trade-off between controlling the fineness of the nanostructures and the fabrication complication. Popular random patterned nanostructures include physical deposition followed by thermal annealing, electrochemical deposition and chemical nanostructure synthesis followed by coating, etc. The fabrication processes for these methods are relatively easy, although the pattern parameters cannot be fully controlled.

The deposition-annealing method to fabricate metal nanoparticles is popular due to its simplicity and capacity to upscale for mass production. In this method a metal thin-film was deposited directly on the solar cell surface, followed by a thermal annealing process at about 200°C to transform the metal film into nanoparticles. Reported deposition methods for plasmonic solar cells include thermal evaporation [10, 12, 16, 20, 24, 34, 79, 80, 81], electron-beam evaporation [46] and sputtering [16]. With deposited film thickness the same, evaporation and sputtering were found to produce identical nanoparticles [16]. Although all the deposition methods involve vacuum, it is not evident the processing pressure to be an important parameter for the performance of solar cells, i.e., low vacuum or atmospheric deposition may be applicable. One significant advantage of the deposition-annealing method is deposition and annealing tools are suitable for in-line mass production; but this method is much limited by the control of the nanoparticles, i.e., it is impossible to use one controlling factor, film thickness, to independently control the particle size, shape and packing density. Also, a uniform array of nanoparticle diameter less than 100 nm is difficult to realize, unless ultra-slow and costly deposition methods are used, e.g., molecular beam epitaxy or atomic layer deposition.

Depositing metal flux through a patterned mask can save the annealing process and achieve an accurate pattern as designed [19, 82]. The aperture of the mask can determine the horizontal shape of the deposited nanostructures, and the deposition thickness can control the height. Mass production of this technology requires high reliability and long lifetime

of the template. Thinner templates tend to be more fragile; thicker templates tend to clog more easily by the deposited material.

Electrodeposition of metal nanoparticles usually involves an electrically assisted reduction of metal cations in a solution environment. Electrodeposition of Ag nanoparticles for plasmonic light enhancement for PV devices has been reported [83, 84]. Electrodeposited metal nanoparticles can be relatively small in size but densely packed. However, uniform nanoparticle deposition requires accurate control of the potential over the entire surface area, which can be challenging. Also, a prerequisite of the electrodeposition is to have potential applied on electrodes of the solar cell. For wafer-based and most of the layer-transfer solar cells, metallization (electrodes formation) is within the last steps of the entire fabrication sequence, thus in this case the electrodeposition process has to limited to the very end.

Metal nanostructures can be chemically synthesized and coated on PV devices. The synthesis process of metal nanodots and nanospheres generally involves chemical reactions, which reduce the targeting metal cations from the metal salt solutions, followed by steps of controlled precipitation and stabilization of the colloids [85–89]. More complex shapes, like Ag nanorods [90], Ag nanowires [89], Au nanorods [88, 91], thorny shaped Au nanoparticles [92], Ag nanoshells [93], nucleated Ag nanoparticles [18], can be synthesized from their respective seeds. For some methods templates have to be used in order to let the seeds grow in the preferential directions, although the template-less methods are preferable, as the template removal steps can be saved. It is also reported that laser ablation can produce Au nanoparticles and form nanonetworks [94], although the productivity seems to be questionable.

The chemically prepared metal nanostructures are then coated on the PV devices. Spin coating [95–97] and drop casting [18, 98, 99] have been widely reported. We recently demonstrated dip coating to be an ideal integration method of Au nanoparticles on commercial screen-printed multicrystalline Si (multi-Si) wafer solar cells [13]. Noticeable advantages of dip coating include the avoidance of vacuum, adjustable nanoparticle packing density through withdrawal speed, uniform particle distribution over large area and applicability for batch-type mass production.

The method of chemical synthesis plus coating can provide more controllable metal nanoparticles, compared with other methods that produce random arrays of nanoparticles. This is because the particle shape, size and packing density can be controlled independently by a series of processing parameters such as synthesis conditions, screening conditions (centrifugation), coating conditions, etc. [13] It is also interesting to notice that the deposition-annealing methods tend to produce hemispherical shaped nanoparticles with a flat surface contacting the substrate, and the chemical synthesis methods are preferable to produce spherical shaped nanoparticles. We found that the plasmonic features of the spherical and hemispherical nanoparticles can be significantly different. Figure 4 shows FDTD simulated scattering patterns of an Ag sphere and a hemisphere on a c-Si substrate

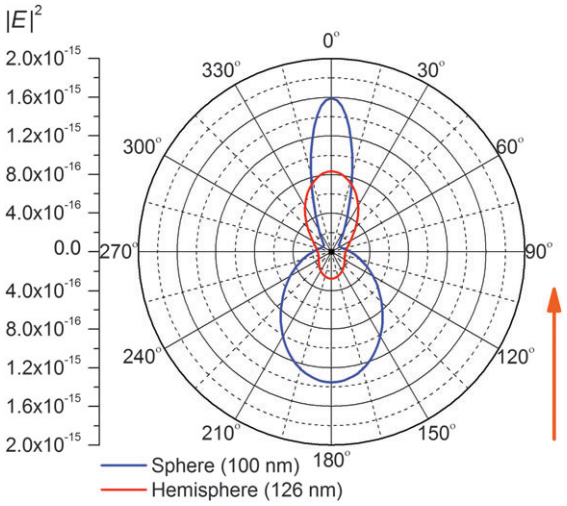

Figure 4 Scattering patterns of the electric field of a Ag sphere (blue) and hemisphere (red) on a c-Si substrate, with diameters 100 and 126 nm respectively, corresponding to the same volume. The arrow indicates the incident white light (300–200 nm) direction.

with diameters of 100 and 126 nm, respectively. The diameters were chosen so that each structure contained identical material volume. In terms of the ability for light scattering, the sphere is considerably better than the hemisphere, indicated by the larger electric field intensity overall. In terms of the light direction, a large amount of the light is reflected backwards for the sphere, while most of the light is forward scattered for the hemisphere. As a result, the hemisphere and deposition-annealing methods may be more suitable for occasions where forward scattering is critical (e.g., front-located nanoparticles), while the sphere and chemical synthesis methods may be more suitable for occasions where strong scattering is more important (e.g., rear-located nanoparticles).

4.2. Ordered structures

Full control of nanoplasmonics for PV devices requires ordered nanostructures, popularly fabricated by lithography technologies. Conventional photolithography is not preferable due to the constraint of the light diffraction limit to the pattern resolution. Instead, electron beam lithography (EBL) and ion beam lithography (IBL) are developed to make high-resolution nanoscale patterns. Although EBL has been reported to directly pattern the metal plasmonic nanostructures on PV devices [100, 101], this method is unlikely to be commercialized due to its extremely low throughput.

Instead, the EBL and IBL are widely used to pattern the mold for nanoimprinting lithography (NIL). In the NIL process, an EBL or IBL defined mold is stamped repeatedly on to a number of cheap resist layers with the pattern precisely transferred to the latter, and finally each replica resist layer is used to pattern a metal nanostructure [102, 103] which is used on a solar cell. NIL-based approaches include: (i) deposit a

metal layer and a resist layer on the PV device, use NIL to pattern the resist layer, and finally etch off part of the metal according to the resist pattern. (ii) Deposit a resist layer on top of the PV device, use NIL to pattern the resist, deposit a metal layer, and finally lift-off part of the metal according to the resist pattern [104]. (iii) Deposit a metal layer on top of a patterned stamp (usually flexible), laminate the stamp on the PV device, peel the stamp off, and leave behind the patterned metal layer on the device surface [105, 106]. (iv) Deposit a resist layer on top of a substrate, use NIL to pattern the resist layer, deposit the metal layer, and finally deposit the PV device on the substrate with the resist left on [17, 106–109]. Approach (iii) is likely to be particularly welcome by the industry, as the metal nanostructures are directly transferred on to the PV device without the resist deposition and etching processes. Approach (iv) is suitable for solar cells whose active layers are deposited or grown on substrates. The NIL stamps can be made of hard or soft materials. Soft stamps are of particular interest for two reasons: first, the soft stamps can form conformal contact to the rough solar cell surfaces and transform patterns precisely without loss, in contrast the hard stamps cannot contact the low-lying areas if the surface is not perfectly flat. Second, the soft stamps can be used on a product line with an in-line roll-to-roll imprinting machine [105, 106], whose ultra-high throughput is preferred by the PV industry.

Other emerging technologies for preparing ordered plasmonic micro or nanostructures, such as colloidal lithography (CL) and block copolymer lithography (BCL), generally involve self-assembled lithographic templates. For the CL, the colloidal particles dispersed orderly in a liquid medium are coated on the surface of the device. The metal can be then deposited either before or after removing the colloidal particles, resulting in positive or negative patterns, respectively [110]. It has been applied for plasmon-enhanced organic PV devices [111]. For the BCL technology, the block copolymers comprise two dissimilar polymer chains that are linked by the covalent force. These chains self-assembles into various morphologies (sphere, cylinders, etc.) in nanoscale, controlled by the volume fraction of the components. The two polymer components are designed to allow one polymer to be more etching-resistive than the other one. So after the etching step, the nanopatterned template is formed [112]. The PV application of the BCL has been proposed [113].

5. Progress in nanoplasmonic photovoltaics

Explosive progress in nanoplasmonic PV has been made during the last few years. Some publications containing experimentally confirmed enhancements on light absorption, photocurrent and energy conversion efficiency are outlined in this section and summarized in Table 1.

Because of the dominating position of wafer-based crystalline Si solar cells in the world PV market, nanoplasmonic research on this type of cell is of significant values. A 7-fold photocurrent enhancement for 300 μm planar wafer c-Si solar cells at the wavelength of 1200 nm and up to 16-fold enhancement at 1050 nm for 1.25 μm silicon-on-insulator solar cells were achieved due to the front-located Ag nanoparticles made by the deposition-annealing method [10]. A 16% photocurrent enhancement from 900 to 1200 nm were achieved by a combined BSR made of Ag nanoparticles and detached Ag mirror [11]. A 10% photocurrent enhancement for 22 μm planar c-Si solar cells was found due to rear-located Ag nanoparticles made by the deposition-annealing method [12]. We recently reported an 11% photocurrent enhancement at the wavelength of 1150 nm and 1.9% (relative) efficiency enhancement for commercial multi-Si wafer solar cells due to the front-located plasmonic Au nanoparticles made by the chemical synthesis and dip-coating method [13]. We have also demonstrated up to 35.2% efficiency enhancement for commercial monocrystalline Si wafer solar cells without surface texture due to simultaneous enhancements in the photocurrent generation and the series conductance through the electrolessly deposited of Ag plasmonic nanoparticles on the ARC and nanoshells on the metal fingers of the cells [14]. It has been found that this method can also further increase the efficiency of the best performing textured solar cells from 18.3% to 19.2%, producing the highest efficiency cells exceeding the state-of-the-art efficiency of the standard screen-printed solar cells [14].

Plasmonic research has been heavily directed to Si-based thin-film solar cells to address the issue of insufficient absorption of light. An 8.1% photocurrent enhancement and 8.3% (relative) efficiency enhancement for substrate-configured thin-film a-Si solar cells were observed attributed to the front-located plasmonic Au nanoparticles made by the synthesis and coating method [15]. A 20% photocurrent enhancement from 10.07 to 12.12 mA/cm^2 for substrate-configured thin-film a-Si solar cells was observed due to the rear-located plasmonic Ag nanoparticles made by the deposition-annealing method [16]. A photocurrent enhancement from 11.52 to 16.94 mA/cm^2 and efficiency enhancement from 6.32% to 9.6% for substrate-configured a-Si thin-film solar cells were observed due to the rear-located Ag nanostructure made by the NIL method [17]. A 44% photocurrent enhancement from 14.85 to 21.42 mA/cm^2 for superstrate-configured polycrystalline Si (poly-Si) thin-film solar cells was reported and the enhancement was attributed to a BSR made of a layer of plasmonic Ag array and white paint [24]. We recently achieved a 14.3% photocurrent enhancement and 23% (relative) efficiency enhancement for superstrate-configured, commercial a-Si thin-film solar cells by using the rear-located Ag nucleated nanoparticles, resulting a final efficiency of 8.1% [18].

For a-Si/c-Si heterojunction solar cells, a 20% photocurrent enhancement from 19 to 22.9 mA/cm^2 and 25% (relative) efficiency enhancement from 7.5% to 9.4% were reported and the enhancements were attributed to the plasmonic effect of the front-located Au nanoparticles made by high temperature sputtering [23]. For GaAs solar cells, a photocurrent enhancement from 11 to 11.9 mA/cm^2 and an efficiency enhancement from 4.7% to 5.9% were achieved with a front-located array of Ag nanoparticles made by evaporating Ag through an anodic aluminum oxide template [19].

Most of the reported nanoplasmonic organic solar cells use P3HT:PCBM as an active layer, since this type of solar cell is among the highest-efficient organic solar cells [114]. A 58% photocurrent enhancement from 4.6 to 7.3 mA/cm^2 and an efficiency enhancement from 1.3% to 2.2% were achieved using the front-located Ag nanoparticles made from Ag salt decomposition and spin coating [20]. A photocurrent enhancement from 8.95 to 10.18 mA/cm^2 and an efficiency enhancement from 3.48% to 4.19% were observed when blending the front-located Au nanoparticles made by a chemical synthesis method [115]. By electrostatically assembling a layer of Au nanodots in front of the active layer, a photocurrent enhancement from 10.74 to 11.13 mA/cm^2 and an efficiency enhancement from 3.04% to 3.65% were achieved [21]. Noticeably, the reported nanoparticle sizes for organic solar cells are small in general, because the P3HT:PCBM active layer has absorption band edge around 650 nm, shorter than that of Si and GaAs based semiconductors.

6. Emerging nanoplasmonic technologies

6.1. Advanced plasmonic technologies for solar cell applications

Besides the nanomaterials and nanostructures mentioned in the previous sections, the advances of novel plasmonic nanostructures, including metallic photonic crystals (MPCs), hybrid photonic crystals (HPCs), metamaterials and metallic nanohole arrays with extraordinary transmission, have stimulated the new design of plasmonic solar cells. Some of these new architectures have already led to solar cell performance improvement; some are still in the early stage of proof of the concept.

The MPCs, also known as plasmonic crystals, are able to both diffract the photons and concentrate the light in the near-field region within the active layer of the cells, leading to enhanced light absorption near the band edge of the semiconductor active layer. The MPCs have been proposed to function as the BSR of a-Si solar cells [116]. Absorption simulation showed a potential for such MPC BSR to overcome the $4n^2$ limit at wavelengths from 740 to 800 nm, and experimentally such BSR can achieve an average increase of absorption of 7%–8% [117].

Recently HPCs consisting of dielectric cores covered with metallic nanoshells have been proposed to be able to produce tailored absorption channels suitable for PV applications [118–120]. The absorption channels have narrow bandwidth. However, their strength and wavelengths can be readily tuned by varying the dimensions of the core and the shells, providing a novel approach for multi-channel operation. It has been found by changing the geometry of the building blocks of these HPCs from elliptical to rectangular shape, the absorption can reach almost unity [119]. Although the application of such HPCs in PV has yet to be explored, the great potential of this new concept is worth noticing.

Metamaterials as one of the most active branches of plasmonic research has recently received enormous attention. The application of metamaterials in PV has also been proposed [121–125]. Theoretical work has been proposed and demonstrated on embedding a planar 20 nm-thick fishnet metamaterial structure in the rear passivation layer of a-Si thin-film solar cells for enhancing the efficiency [126]. By matching the input impedance to reduce the reflection and exciting the plasmon resonance of the metamaterial, light absorption near the bandgap of the a-Si active layer was enhanced by 12 times at the normal incidence. As much as 64% of the total absorbed energy at resonance is in the silicon layer, which led to a 14.8% photocurrent enhancement near the bandgap of the a-Si and an 16.8% (relative) efficiency enhancement from 6.36% to 7.43%.

Periodic arrays of metallic nanoholes facilitating extraordinary transmission was also proposed to be used as the back electrodes to produce propagating surface plasmon waves for improving the generation of charge carriers. Such nanohole array was fabricated in Au films by using a lithography technology. The diameter and periodicity of the hole and the thickness of the metal film can be well controlled to achieve optimized plasmonic resonance. A photocurrent enhancement has been demonstrated in polymer solar cells [127].

6.2. Plasmonic effect enabled revolution of solar cell technologies

Plasmonic nanostructures offer new mechanisms for enhancing the performance of solar cells. This has in turn led to the revolution of the solar cell design. For example, it is affordable to reduce the active layer for all types of PV devices with the advanced plasmonic light absorption enhancement. In a-Si thin-film solar cells, the use of plasmonic nanostructured rear contact enabled the dramatic reduction of the thickness of the active layer [17, 109]. The thickness reduction offers cost reduction and cell stabilized performance improvement, due to the reduction of the bulk contribution of the light-induced metastable defects which are proportional to the volume of the a-Si layer [128]. In addition, the active layer of PV devices should be fabricated in a way that the nanoplasmonic structures can be embedded, enabling ultra-high light absorption enhancements.

Although still in its infancy, nanoplasmonic PV have already shown a great potential in dramatically boosting the device performance. A number of high efficiency cell concepts have been proposed and some of them have already demonstrated considerable efficiency enhancement. The advances of the field hold great promises for revolutionary PV technologies of both high efficiency and low cost. Despite of the great potential of these novel plasmonic solar cells, key fundamental and technical challenges need to be addressed before they could become practically useful, including narrow bandwidth, angle and polarization dependence, and expensive and sophisticated fabrication techniques for nanostructures, with some solutions have been addressed or proposed in this paper.

Acknowledgements

The authors acknowledge the financial support from the Victorian Government to establish the Victoria-Suntech Advanced Solar Facility (VSASF) under the Victoria Science Agenda (VSA) scheme. B.J. thanks the Victorian Government for the support through the Victorian Fellowship.

References

[1] Blankenship RE, Tiede DM, Barber J, Brudvig GW, Ort DR, Parson WW, Prince RC, Sayre RT. Comparing photosynthetic and photovoltaic efficiencies and recognizing the potential for improvement. Science 2011;332:805–9.
[2] Mills D. Advances in solar thermal electricity technology. Sol Energy 2004;76:19–31.
[3] Chapin DM, Fuller CS, Pearson GL. A new silicon p-n Junction photocell for converting solar radiation into electrical power. J Appl Phys 1954;25:676–7.
[4] Zhao J, Wang A, Green MA, Ferrazza F. 19.8% efficient "honeycomb" textured multicrystalline and 24.4% monocrystalline silicon solar cells. Appl Phys Lett 1998;73:1991–3.
[5] Yablonovitch E, Cody GD. Intensity enhancement in textured optical sheets for solar cells. IEEE T Electron Dev 1982;29:300–5.
[6] Campbell P, Green MA. Light trapping properties of pyramidally textured surfaces. J Appl Phys 1987;62:243–9.
[7] Yu Z, Raman A, Fan S. Fundamental limit of nanophotonic light trapping in solar cells. Proc Natl Acad Sci USA 2010;107:17491–6.
[8] Callahan DM, Munday JN, Atwater HA. Solar cell light trapping beyond the ray optic limit. Nano Lett 2011;12:214–8.
[9] Atwater HA, Polman A. Plasmonics for improved photovoltaic devices. Nat Mater 2010;9:205–13.
[10] Pillai S, Catchpole KR, Trupke T, Green MA. Surface plasmon enhanced silicon solar cells. J Appl Phys 2007;101:093105.
[11] Yang Y, Pillai S, Mehrvarz H, Kampwerth H, Ho-Baillie A, Green MA. Enhanced light trapping for high efficiency crystalline solar cells by the application of rear surface plasmons. Sol Energ Mat Sol C 2012;101:217–26.
[12] Beck FJ, Mokkapati S, Catchpole KR. Plasmonic light-trapping for Si solar cells using self-assembled, Ag nanoparticles. Prog Photovoltaics 2010;18:500–4.
[13] Fahim N, Ouyang Z, Zhang Y, Baohua J, Zhengrong S, Min G. Efficiency enhancement of screen-printed multicrystalline silicon solar cells by integrating gold nanoparticles via a dip coating process. Opt Mater Express 2012;2:190–204.
[14] Fahim N, Jia B, Shi Z, Gu M. Simultaneous broadband light trapping and fill factor enhancement in crystalline silicon solar cells induced by Ag nanoparticles and nanoshells. Opt Express 2012;20:A694–A705.
[15] Derkacs D, Lim SH, Matheu P, Mar W, Yu ET. Improved performance of amorphous silicon solar cells via scattering from surface plasmon polaritons in nearby metallic nanoparticles. Appl Phys Lett 2006;89:093103–3.
[16] Eminian C, Haug F-J, Cubero O, Niquille X, Ballif C. Photocurrent enhancement in thin film amorphous silicon solar cells with silver nanoparticles. Prog Photovoltaics 2011;19:260–5.
[17] Ferry VE, Verschuuren MA, van Lare C, Ruud EI, Atwater HA, Polman A. Optimized spatial correlations for broadband light trapping nanopatterns in high efficiency ultrathin film a-Si:H solar cells. Nano Lett 2011;11:4239–45.
[18] Chen X, Jia B, Saha JK, Cai B, Stokes N, Qiao Q, Wang Y, Shi Z, Gu M. Broadband enhancement in thin-film amorphous silicon solar cells enabled by nucleated silver nanoparticles. Nano Lett 2012;12:2187–92.
[19] Nakayama K, Tanabe K, Atwater HA. Plasmonic nanoparticle enhanced light absorption in GaAs solar cells. Appl Phys Lett 2008;93:121904–3.
[20] Morfa AJ, Rowlen KL, Reilly III TH, Romero MJ, van de Lagemaat J. Plasmon-enhanced solar energy conversion in organic bulk heterojunction photovoltaics. Appl Phys Lett 2008;92:013504.
[21] Lee JH, Park JH, Kim JS, Lee DY, Cho K. High efficiency polymer solar cells with wet deposited plasmonic gold nanodots. Org Electron 2009;10:416–20.
[22] Rockstuhl C, Fahr S, Lederer F. Absorption enhancement in solar cells by localized plasmon polaritons. J Appl Phys 2008;104:123102–7.
[23] Losurdo M, Giangregorio MM, Bianco GV, Sacchetti A, Capezzuto P, Bruno G. Enhanced absorption in Au nanoparticles/a-Si:H/c-Si heterojunction solar cells exploiting Au surface plasmon resonance. Sol Energ Mat Sol C 2009;93:1749–54.
[24] Ouyang Z, Zhao X, Varlamov S, Tao Y, Wong J, Pillai S. Nanoparticle-enhanced light trapping in thin-film silicon solar cells. Prog Photovoltaics 2011;19:917–26.
[25] Wang J-Y, Tsai F-J, Huang J-J, Chen CY, Li N, Kiang YW, Yang CC. Enhancing InGaN-based solar cell efficiency through localized surface plasmon interaction by embedding Ag nanoparticles in the absorbing layer. Opt Express 2010;18:2682–94.
[26] Rand BP, Peumans P, Forrest SR. Long-range absorption enhancement in organic tandem thin-film solar cells containing silver nanoclusters. J Appl Phys 2004;96:7519–26.
[27] Tvingstedt K, Persson N-K, Inganas O, Rahachou A, Zozoulenko IV. Surface plasmon increase absorption in polymer photovoltaic cells. Appl Phys Lett 2007;91:113514–3.
[28] Ouyang Z. Electron-beam evaporated polycrystalline silicon thin-film solar cells: paths to better performance. University of New South Wales, Sydney, 2011.
[29] Green MA. Enhanced evanescent mode light trapping in organic solar cells and other low index optoelectronic devices. Prog Photovoltaics 2011;19:473–7.
[30] Bohren CF, Huffman DR. Absorption and scattering of light by small particles. Wiley-Interscience: New York, 1998.
[31] Catchpole KR, Polman A. Design principles for particle plasmon enhanced solar cells. Appl Phys Lett 2008;93:191113–3.
[32] Ferry VE, Munday JN, Atwater HA. Design considerations for plasmonic photovoltaics. Adv Mater 2010;22:4794–808.
[33] Stuart HR, Hall DG. Absorption enhancement in silicon-on-insulator waveguides using metal island films. Appl Phys Lett 1996;69:2327–9.
[34] Stuart HR, Hall DG. Island size effects in nanoparticle-enhanced photodetectors. Appl Phys Lett 1998;73:3815–7.
[35] Beck FJ, Polman A, Catchpole KR. Tunable light trapping for solar cells using localized surface plasmons. J Appl Phys 2009;105:114310–7.
[36] Pillai S, Beck FJ, Catchpole KR, Ouyang Z, Green MA. The effect of dielectric spacer thickness on surface plasmon enhanced solar cells for front and rear side depositions. J Appl Phys 2011;109:073105.
[37] Beck FJ, Mokkapati S, Polman A, Catchpole KR. Asymmetry in photocurrent enhancement by plasmonic nanoparticle arrays located on the front or on the rear of solar cells. Appl Phys Lett 2010;96:033113–3.

[38] Temple TL, Bagnall DM. Broadband scattering of the solar spectrum by spherical metal nanoparticles. Prog Photovoltaics 2012, DOI: 10.1002/pip.237.
[39] Sheng X, Johnson SG, Michel J, Kimerling LC. Optimization-based design of surface textures for thin-film Si solar cells. Opt Express 2011;19:A841–A50.
[40] Ferry VE, Sweatlock LA, Pacifici D, Atwater HA. Plasmonic nanostructure design for efficient light coupling into solar cells. Nano Lett 2008;8:4391–7.
[41] Catchpole KR. Nanostructures in photovoltaics. Phil Trans R Soc A 2006;364:3493–503.
[42] Zhu J, Li J-J, Zhao J-W. Tuning the wavelength drift between resonance light absorption and scattering of plasmonic nanoparticle. Appl Phys Lett 2011;99:101901–3.
[43] Qu D, Liu F, Yu J, Huan Y, Xie W, Xu Q. Plasmonic core-shell gold nanoparticle enhanced optical absorption in photovoltaic devices. Appl Phys Lett 2011;98:113119–3.
[44] Ouyang Z, Pillai S, Beck F, Kunz O, Varlamov S, Catchpole KR, Campbell P, Green MA. Effective light trapping in polycrystalline silicon thin-film solar cells by means of rear localized surface plasmons. Appl Phys Lett 2010;96:261109–3.
[45] Zhang Y, Ouyang Z, Stokes N, Jia B, Shi Z, Gu M. Low cost and high performance Al nanoparticles for broadband light trapping in Si wafer solar cells. Appl Phys Lett 2012;100:151101–4.
[46] Temple TL, Mahanama GDK, Reehal HS, Bagnall DM. Influence of localized surface plasmon excitation in silver nanoparticles on the performance of silicon solar cells. Sol Energ Mat Sol C 2009;93:1978–85.
[47] Hägglund C, Apell SP. Resource efficient plasmon-based 2D-photovoltaics with reflective support. Opt Express 2010;18:A343–A56.
[48] Hägglund C, Apell SP. Plasmonic near-field absorbers for ultrathin solar cells. J Phys Chem Lett 2012;3:1275–85.
[49] Green MA. Solar cells: operating principles, technology and system applications. University of New South Wales: Kensington, NSW, 1998; p 274.
[50] Sze SM, Ng KK. Physics of semiconductor devices. 3rd ed.; John Wiley & Sons, Inc.: Hoboken, NJ, 2007; p 815.
[51] Zhu J, Xue M, Shen H, Wu Z, Kim S, Ho JJ, Hassani-Afshar A, Zeng B, Wang KL. Plasmonic effects for light concentration in organic photovoltaic thin films induced by hexagonal periodic metallic nanospheres. Appl Phys Lett 2011;98:151110–3.
[52] Beck FJ, Verhagen E, Mokkapati S, Polman A, Catchpole KR. Resonant SPP modes supported by discrete metal nanoparticles on high-index substrates. Opt Express 2011;19:A146–A56.
[53] Pala RA, White J, Barnard E, Liu J, Brongersma ML. Design of plasmonic thin-film solar cells with broadband absorption enhancements. Adv Mater 2009;21:3504–9.
[54] Springer J, Poruba A, Mullerova L, Vanecek M, Kluth O, Rech B. Absorption loss at nanorough silver back reflector of thin-film silicon solar cells. J Appl Phys 2004;95:1427–9.
[55] Franken RH, Stolk RL, Li H, van der Werf CHM, Rath JK, Schropp REL. Understanding light trapping by light scattering textured back electrodes in thin film n-i-p-type silicon solar cells. J Appl Phys 2007;102:7.
[56] Schropp REI, Li H, Franken RHJ, Rath JK, van der Werf CHM, Schüttauf JA, Stolk RL. Nanostructured thin films for multibandgap silicon triple junction solar cells. Sol Energ Mat Sol C 2009;93:1129–33.
[57] Kim Y, Jung S, Ju M, Ryua K, Parka J, Choi H, Yang D, Lee Y, Yi J. The effect of rear surface polishing to the performance of thin crystalline silicon solar cells. Sol Energy 2011;85:1085–90.
[58] Bai W, Gan Q, Bartoli F, Zhang J, Cai L, Huang Y, Song G. Design of plasmonic back structures for efficiency enhancement of thin-film amorphous Si solar cells. Opt Lett 2009;34:3725–7.
[59] Mokkapati S, Beck FJ, Polman A, Catchpole KR. Designing periodic arrays of metal nanoparticles for light-trapping applications in solar cells. Appl Phys Lett 2009;95:053115–3.
[60] Spinelli P, Hebbink M, de Waele R, Black L, Lenzmann F, Polman A. Optical impedance matching using coupled plasmonic nanoparticle arrays. Nano Lett 2011;11:1760–5.
[61] Sha WEI, Choy WCH, Chew WC. A comprehensive study for the plasmonic thin-film solar cell with periodic structure. Opt Express 2010;18:5993–6007.
[62] Lim SH, Mar W, Matheu P, Derkacs D, Yu ET. Photocurrent spectroscopy of optical absorption enhancement in silicon photodiodes via scattering from surface plasmon polaritons in gold nanoparticles. J Appl Phys 2007;101:104309–7.
[63] Shen H, Bienstman P, Maes B. Plasmonic absorption enhancement in organic solar cells with thin active layers. J Appl Phys 2009;106:073109–5.
[64] Akimov YA, Ostrikov K, Li EP. Surface plasmon enhancement of optical absorption in thin-film silicon solar cells. Plasmonics 2009;4:107–13.
[65] Yee K. Numerical solution of initial boundary value problems involving maxwell's equations in isotropic media. IEEE T Antenn Propag 1966;14:302–7.
[66] Zhao J, Pinchuk AO, McMahon JM, Li S, Ausman LK, Atkinson AL, Schatz GC. Methods for describing the electromagnetic properties of silver and gold nanoparticles. Accounts Chem Res 2008;41:1710–20.
[67] FDTD Solutions. http://www.lumerical.com.
[68] Mokkapati S, Beck FJ, Waele Rd, Polman A, Catchpole KR. Resonant nano-antennas for light trapping in plasmonic solar cells. J Phys D Appl Phys 2011;44:185101.
[69] COMSOL Multiphysics. http://www.comsol.com.
[70] Akimov YA, Koh WS. Resonant and nonresonant plasmonic nanoparticle enhancement for thin-film silicon solar cells. Nanotechnology 2010;21:235201.
[71] Akimov Y, Koh W. Design of Plasmonic nanoparticles for efficient subwavelength light trapping in thin-film solar cells. Plasmonics 2011;6:155–61.
[72] Wang W, Wu S, Reinhardt K, Lu Y, Chen S. Broadband light absorption enhancement in thin-film silicon solar cells. Nano Lett 2010;10:2012–8.
[73] ATLAS. http://www.silvaco.com/.
[74] Clugston DA, Basore PA In 32-Bit solar cell modeling on personal computers, 26th IEEE Photovoltaic Specialists Conference, Anaheim, CA, October, 1997; Anaheim, CA, 1997; pp 207–10.
[75] Tao Y, Varlamov S, Kunz O, Ouyang Z, Wong J, Soderstrom T, Wolf M, Egan R. Effects of annealing temperature on crystallisation kinetics, film properties and cell performance of silicon thin-film solar cells on glass. Sol Energ Mat Sol C 2012.
[76] Basic Research Needs for Solar Energy Utilization; U.S. Department of Energy: Washington DC, 18–21 April, 2005.
[77] Lewis NS. Toward cost-effective solar energy use. Science 2007;315:798–801.
[78] Green MA. Third generation photovoltaics: advanced solar energy conversion. Springer: New York, 2003.
[79] Yang L, Li X, Tuo X, Van Nguyen TT, Luo X, Hong M. Alloy nanoparticle plasmon resonance for enhancing broadband

antireflection of laser-textured silicon surfaces. Opt Express 2011;19:A657–A63.
[80] Luo PQ, Moulin E, Sukmanowski J, Royer FX, Dou XM, Stiebig H. Enhanced infrared response of ultra thin amorphous silicon photosensitive devices with Ag nanoparticles. Thin Solid Films 2009;517:6256–9.
[81] Westphalen M, Kreibig U, Rostalski J, Lüth H, Meissner D. Metal cluster enhanced organic solar cells. Sol Energ Mat Sol C 2000;61:97–105.
[82] Masuda H, Satoh M. Fabrication of gold nanodot array using anodic porous alumina as an evaporation mask. Jpn J Appl Phys 1996;35:L126.
[83] Kim S-S, Na S-I, Jo J, Kim D-Y, Nah Y-C. Plasmon enhanced performance of organic solar cells using electrodeposited Ag nanoparticles. Appl Phys Lett 2008;93:073307–3.
[84] Sakai N, Fujiwara Y, Takahashi Y, Tatsuma T. Plasmon-resonance-based generation of cathodic photocurrent at electrodeposited gold nanoparticles coated with TiO2 films. ChemPhysChem 2009;10:766–9.
[85] Evans DF, Wennerström H. The collidal Domain: where physics, chemistry, and technology meet. 2nd ed.; Wiley-VCH: New York, 1999.
[86] Frens G. Controlled nucleation for the regulation of the particle size in monodisperse gold suspensions. Nat Phys Sci 1973;241:20–2.
[87] Brown KR, Walter DG, Natan MJ. Seeding of colloidal Au nanoparticle solutions. 2. Improved control of particle size and shape. Chem Mater 1999;12:306–13.
[88] Jana NR, Gearheart L, Murphy CJ. Wet chemical synthesis of high aspect ratio cylindrical gold nanorods. J Phys Chem B 2001;105:4065–7.
[89] Zhang D, Qi L, Yang J, Ma J, Cheng H, Huang L. Wet chemical synthesis of silver nanowire thin films at ambient temperature. Chem Mater 2004;16:872–6.
[90] Jana NR, Gearheart L, Murphy CJ. Wet chemical synthesis of silver nanorods and nanowires of controllable aspect ratio. Chem Commun 2001.
[91] Nikoobakht B, El-Sayed MA. Preparation and growth mechanism of gold nanorods (NRs) using seed-mediated growth method. Chem Mater 2003;15:1957–62.
[92] Yuan H, Ma W, Chen C, Zhao J, Liu J, Zhu H, Gao X. Shape and SPR evolution of thorny gold nanoparticles promoted by silver ions. Chem Mater 2007;19:1592–600.
[93] Sun Y, Xia Y. Mechanistic study on the replacement reaction between silver nanostructures and chloroauric acid in aqueous medium. J Am Chem Soc 2004;126:3892–901.
[94] Mafune F, Kohno J-y, Takeda Y, Kondow T. Formation of gold nanonetworks and small gold nanoparticles by irradiation of intense pulsed laser onto gold nanoparticles. J Phys Chem B 2003;107:12589–96.
[95] Duche D, Torchio P, Escoubas L, Monestier F, Simon JJ, Flory F, Mathian G. Improving light absorption in organic solar cells by plasmonic contribution. Sol Energ Mat Sol C 2009;93:1377–82.
[96] Wan D, Chen H-L, Tseng T-C, Fang CY, Lai YS, Yeh FY. Antireflective nanoparticle arrays enhance the efficiency of silicon solar cells. Adv Funct Mater 2010;20:3064–75.
[97] Yoon W-J, Jung K-Y, Liu J, Duraisamy T, Revur R, Teixeira FL, Sengupt S, Berger PR. Plasmon-enhanced optical absorption and photocurrent in organic bulk heterojunction photovoltaic devices using self-assembled layer of silver nanoparticles. Sol Energ Mat Sol C 2010;94:128–32.
[98] Schaadt DM, Feng B, Yu ET. Enhanced semiconductor optical absorption via surface plasmon excitation in metal nanoparticles. Appl Phys Lett 2005;86:063106–3.
[99] Matheu P, Lim SH, Derkacs D, McPheeters C, Yu ET. Metal and dielectric nanoparticle scattering for improved optical absorption in photovoltaic devices. Appl Phys Lett 2008;93:113108.
[100] Hägglund C, Zach M, Petersson G, Kasemo B. Electromagnetic coupling of light into a silicon solar cell by nanodisk plasmons. Appl Phys Lett 2008;92:053110.
[101] Hägglund C, Zach M, Kasemo B. Enhanced charge carrier generation in dye sensitized solar cells by nanoparticle plasmons. Appl Phys Lett 2008;92:013113–3.
[102] Guo LJ. Nanoimprint lithography: methods and material requirements. Adv Mater 2007;19:495–513.
[103] Chou SY, Krauss PR, Renstrom PJ. Imprint lithography with 25-nanometer resolution. Science 1996;272:85–7.
[104] Wang E, Mokkapati S, Beck FJ, Ouyang Z, Varlamov S, Catchpole K. In Periodic silver nanoparticles fabricated with soft-stamp nanoimprint on silicon solar cells, 25th european photovoltaic solar energy conference. Valencia, Spain, 2010; Valencia, Spain, 2010.
[105] Kang M-G, Kim M-S, Kim J, Guo LJ. Organic solar cells using nanoimprinted transparent metal electrodes. Adv Mater 2008;20:4408–13.
[106] Kang M-G, Joon Park H, Hyun Ahn S, Jay Guo L. Transparent Cu nanowire mesh electrode on flexible substrates fabricated by transfer printing and its application in organic solar cells. Sol Energ Mat Sol C 2010;94:1179–84.
[107] Söderström K, Escarré J, Cubero O, Haug FJ, Perregaux S, Ballif C. UV-nano-imprint lithography technique for the replication of back reflectors for n-i-p thin film silicon solar cells. Prog Photovoltaics 2011;19:202–10.
[108] Ferry VE, Verschuuren MA, Li HBT, Verhagen E, Walters RJ, Schropp REI, Atwater HA, Polman A. Improved red-response in thin film a-Si:H solar cells with soft-imprinted plasmonic back reflectors. Appl Phys Lett 2009;95:183503–3.
[109] Ferry VE, Verschuuren MA, Li HBT, Verhagen E, Walters RJ, Schropp REI, Atwater HA, Polman A. Light trapping in ultrathin plasmonic solar cells. Opt Express 2010;18:A237–A45.
[110] Yang S-M, Jang SG, Choi D-G, Kim S, Yu HK. Nanomachining by colloidal lithography. Small 2006;2:458–75.
[111] Reilly TH, van de Lagemaat J, Tenent RC, Morfa AJ, Rowlen KL. Surface-plasmon enhanced transparent electrodes in organic photovoltaics. Appl Phys Lett 2008;92:3.
[112] Hawker CJ, Russell TP. Block copolymer lithography: merging, "bottom-up" with "top-down" processes. MRS Bull 2005;30:952–66.
[113] Darling SB. Block copolymers for photovoltaics. Energy Environ Sci 2009;2:1266–73.
[114] Li G, Shrotriya V, Huang J, Yao Y, Moriarty T, Emery K, Yang Y. High-efficiency solution processable polymer photovoltaic cells by self-organization of polymer blends. Nat Mater 2005;4:864–8.
[115] Chen F-C, Wu J-L, Lee C-L, Hong Y, Kuo CH, Huang MH. Plasmonic-enhanced polymer photovoltaic devices incorporating solution-processable metal nanoparticles. Appl Phys Lett 2009;95:013305–3.
[116] Biswas R, Zhou D. Simulation and modelling of photonic and plasmonic crystal back reflectors for efficient light trapping. Physica Status Solidi (A) 2010;207:667–70.
[117] Curtin B, Biswas R, Dalal V. Photonic crystal based back reflectors for light management and enhanced absorption in amorphous silicon solar cells. Appl Phys Lett 2009;95:231102–3.

[118] Li J, Hossain MDM, Jia B, Buso D, Gu M. Three-dimensional hybrid photonic crystals merged with localized plasmon resonances. Opt Express 2010;18:4491–8.
[119] Li J, Hossain MM, Jia B, Gu M. Rectangular-cavity resonances enhanced absorption in metallic-nanoshelled 2D rod arrays and 3D photonic crystals. N J Phys 2010;12:043012.
[120] Hossain MM, Gu M. Broadband optical absorptions in inversed woodpile metallic photonic crystals. Opt Mater Express 2012;2:996–1002.
[121] Enemuo A, Crouse DT, Crouse M. In PN junction fabrication of solar cells and integration with metamaterials, Prague, Czech Republic, Proc. SPIE Metamaterials VI2011; 80700W; doi:10.1117/12.887124.
[122] Varadan VV, Liming J. In Optical metastructures for trapping light in thin Si solar cells, 35th IEEE Photovoltaic Specialists Conference, Honolulu, Hawaii, USA, 20–25 June, 2010; Honolulu, HI, USA, 2010; pp 001057–9.
[123] Alici KB, Ozbay E. In Photonic metamaterial absorber designs for infrared solar cell applications. Proc. SPIE 7772, Next Generation (Nano) Photonic and Cell Technologies for Solar Energy Conversion, 77721B (August 30, 2010); doi:10.1117/12.860223.
[124] Yang J, Huang M, Yang C, Xiao Z, Peng J. Metamaterial electromagnetic concentrators with arbitrary geometries. Opt Express 2009;17:19656–61.
[125] Bagnall DM, Boreland M. Photovoltaic technologies. Energ Policy 2008;36:4390–6.
[126] Ji L, Varadan VV. Fishnet metastructure for efficiency enhancement of a thin film solar cell. J Appl Phys 2011;110: 043114–8.
[127] Menezes JW, Ferreira J, Santos MJL, Cescato L, Brolo AG. Large-Area fabrication of periodic arrays of nanoholes in metal films and their application in biosensing and plasmonic-enhanced photovoltaics. Adv Funct Mater 2010;20:3918–24.
[128] Stutzmann M, Jackson WB, Tsai CC. Light-induced metastable defects in hydrogenated amorphous silicon: a systematic study. Phys Rev B 1985;32:23–47.

Received June 5, 2012; accepted September 13, 2012